

# MOLECULAR DYNAMICS STUDY OF THE NUCLEATION OF BUBBLE

Takashi Tokumasu<sup>1</sup>, Kenjiro Kamiyo<sup>1</sup>, Mamoru Oike<sup>1</sup> and Yoichiro Matsumoto<sup>2</sup>

<sup>1</sup>Tohoku University, Sendai, Miyagi, 980-8577, Japan

<sup>2</sup>The University of Tokyo, Bunkyo-ku, Tokyo, 113-8656, Japan

## Abstract

In this paper the effect of internal degrees of freedom on the limit of metastability is analyzed by the Molecular Dynamics (MD) method. Oxygen is assumed as the liquid and oxygen molecules are assumed as both monatomic and diatomic molecules. The Lennard–Jones (LJ) potential is used as the intermolecular potential for monatomic molecules and 2 Center Lennard–Jones (2CLJ) potential is used as the intermolecular potential for diatomic molecules. These parameters are determined so that the averaged potentials of the respective molecules are consistent with each other. Simulations are performed at various states and an Equation of State (EOS) of each liquid is obtained. The spinodal lines obtained from the respective EOSs are compared with each other and the effect of molecular orientation in diatomic liquid on the thermodynamic limit of metastability is investigated. Moreover, the kinetic limit of metastability is also investigated and the difference between the monatomic and diatomic liquid oxygen is analyzed.

## 1 Introduction

These days there are increasing requirements of bubble nucleation in applications ranging from microdevices to macro–scale hydraulic machinery with regard to such aspects as microbubble actuation (Lin 1998), cavitation (Trevena 1987), etc. Especially in cryogenic fluids, there are fewer foreign molecules than in water and nucleation phenomena are considered to be homogeneous. In this condition, the liquid is superheated and will boil explosively. These boiling may result in serious damage to materials (Blander and Katz 1975). For this reason, it is important to obtain knowledge of the bubble nucleation point in such explosive boiling.

Bubble nucleation in such circumstances is a micro– to nano–scale phenomenon, and it is necessary to use a method which can treat the microscale motion of fluids. The Molecular Dynamics (MD) method is an effective one for analyzing such a microscale phenomenon and, to date, many researchers have analyzed such phenomena using this method (Kinjo and Matsumoto 1998, Tokumasu, Kamiyo, Oike and Matsumoto 2000). The objective of this study, therefore, is to explore the bubble nucleation phenomena microscopically by the MD method. Especially, the effect of the characteristics of diatomic molecules on bubble nucleation is analyzed. Oxygen is assumed as the liquid. Moreover, the bubble nucleation in monatomic liquid whose potential parameters are consistent with those in diatomic liquid is also simulated. These results are compared with each other and the effect of the characteristics of diatomic liquid on the limit of metastability is investigated.

## 2 Molecular Potential

It is necessary to determine the intermolecular potential between oxygen molecules to simulate the bubble nucleation in liquid oxygen. In this paper, the Lennard–Jones (12–6) potential, as follows, is used:

$$\varphi_m = 4\varepsilon_m \left\{ \left( \frac{\sigma_m}{r} \right)^{12} - \left( \frac{\sigma_m}{r} \right)^6 \right\}, \quad (1)$$

where the parameters,  $\sigma_m$  and  $\varepsilon_m$ , are obtained from an experimentally obtained result of viscosity coefficient, assuming that oxygen molecules are monatomic ones. In this paper, these values are determined as  $\sigma_m =$

$3.47 \times 10^{-10}$  m and  $\varepsilon_m = 14.7 \times 10^{-22}$  J (Reid, Prausnitz and Sherwood 1977). However, oxygen molecules are diatomic and their internal degrees of freedom have some effects on bubble nucleation. An oxygen molecule has rotational and vibrational degrees of freedom as the internal one, but it is sufficient to consider the rotational degree of freedom because vibrational one is frozen at such a low temperature. In this paper 2 Center Lennard–Jones (2CLJ) potential (Singer, Taylor and Singer 1977),  $\varphi_a$ , is used to treat the rotational degree of freedom. The potential parameters are determined as follows:

As shown in Fig. 1, the system of the two rigid molecules is expressed by an intermolecular relative position vector  $\mathbf{R} = (R, \Theta, \Phi)$  of the center of the mass of molecule 2 with respect to that of molecule 1 and two interatomic relative position vectors of the diatomic molecule  $i (= 1, 2)$ ,  $\mathbf{r} = (r_i, \theta_i, \phi_i)$ , where  $r_i$  is the interatomic distance. In order to simplify the calculations, we have chosen a special frame with the  $z$  axis

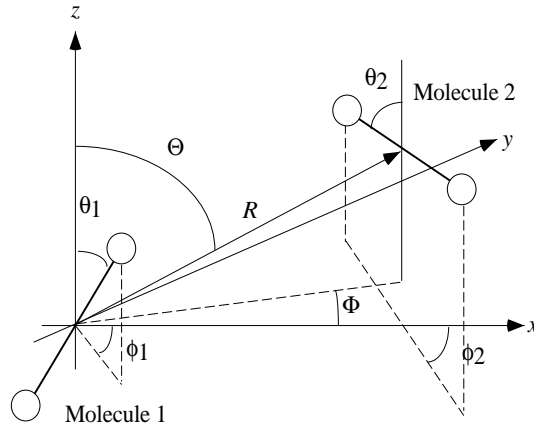


Figure 1: The coordinate system used to calculate the potential parameters

along  $\mathbf{R}$  ( $\Theta = \Phi = 0$ ) and molecule 2 in the  $x - z$  plane ( $\phi_2 = 0$ ). Since the interatomic distance  $r_i$  is invariant, only the internal coordinates  $R$ ,  $\theta_1$ ,  $\phi_1$  and  $\phi_2$  are varied. The averaged intermolecular potential is obtained by varying the angular parameters,  $\theta_1$ ,  $\theta_2$  in proportion to  $\cos \theta$  and  $\phi_1$  in proportion to  $\phi$ . The range of  $\theta$  and  $\phi$  are  $0 < \theta < \pi/2$  and  $0 < \phi < 2\pi$ , respectively. Next, the difference of the potential between monatomic and diatomic molecules is obtained by

$$S(\sigma_a, \varepsilon_a) = \int_{R_{min}}^{R_{max}} (\varphi_a - \varphi_m)^2 dR. \quad (2)$$

In this paper, the parameters of the 2CLJ potential are obtained so that the difference becomes minimum. The range of the integral is from  $R_{min} = 3.5 \text{ \AA}$  to  $R_{max} = 7.5 \text{ \AA}$  so that the potential well of the respective potentials are consistent with each other. Consequently, the parameters of the 2CLJ potential are taken to be  $\sigma_a = 2.93 \times 10^{-10}$  m and  $\varepsilon_a = 6.85 \times 10^{-22}$  J, where  $r_i = 1.208 \times 10^{-10}$  m. The potential curve is shown in Fig. 2. As shown in this figure, the averaged potential of diatomic molecules is consistent with that of monatomic molecules. The potentials at some specific orientations are also shown in Fig. 2. As shown in this figure, the potential curve varies well dependent on molecular orientation.

### 3 Thermodynamic Limit of Metastability

The thermodynamic limit of metastability (TLM) at a certain temperature is the point at which the liquid branch of a pressure–density diagram is at a minimum. In order to obtain the TLM, an Equation of State (EOS) of the liquid must be obtained. In this paper the EOS of monatomic and that of diatomic liquid oxygen are obtained by the method of Kataoka (1987) mentioned below.

First, microcanonical MD simulations are carried out in order to obtain the pressure and potential energy at a certain temperature and density. The system treated here consists of  $N = 864$  molecules. The simulations are performed with reduced units, i.e., length  $\sigma_m$ , energy  $\varepsilon_m$  and mass  $m$  (mass of a molecule),

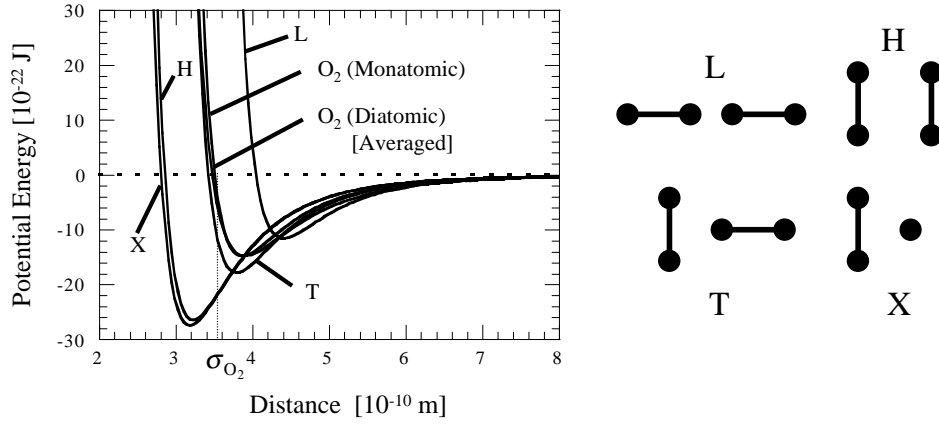


Figure 2: Averaged potential of diatomic oxygen and potentials at each orientation

where  $m = 5.31 \times 10^{-26}$  kg. Thus, the time unit is  $\tau = \sqrt{m\sigma_m/\varepsilon_m}$  and the pressure unit is  $\varepsilon_m/\sigma_m^3$ . For reference, the value of the time unit is 2.09 ps and the value of the pressure unit is 35.2 MPa. The reduced values shown in this paper are those with these reduced units. In this simulation, temperature  $T$  and density  $\rho$  are given and the length of the simulation domain,  $l$ , is obtained by  $l = (N/\rho)^{1/3}$ . A periodic boundary condition is imposed. At the initial condition, the molecules are positioned as a face-centered cubic structure and the velocities of the molecules are obtained by Maxwell distribution at temperature  $T$ . For diatomic molecules, the rotational energies of molecules,  $e_{ri}$ , are also obtained in the same manner and the angular velocity is obtained by  $\omega_i = \sqrt{2e_{ri}/I}$ , where  $I$  is a moment of inertia. The orientations of molecules are given at random. The Verlet scheme is used for time integration and the time step  $\Delta t$  is given by  $\Delta t = 0.0025$ . Quaternions are used for the solution of the orientational equations of motion (Allen and Tildesley 1987). The cutoff distance is determined by  $r_c = 3.5\sigma_m$ . The simulated temperature of the liquid is slightly different from the given temperature. In case of monatomic molecules, it is obtained by

$$T = \frac{2}{3k} \left\langle \sum_{i=1}^N \frac{1}{2} m v_i^2 \right\rangle, \quad (3)$$

and in case of diatomic molecules by

$$T = \frac{2}{5k} \left\langle \sum_{i=1}^N \left( \frac{1}{2} m v_i^2 + \frac{1}{2} I \omega_i^2 \right) \right\rangle, \quad (4)$$

where  $\langle \rangle$  is the average value of the system. The pressure of the liquid is obtained by

$$P = \frac{NkT}{V} + \frac{1}{3V} \left\langle \sum_{i=1}^N \sum_{j>i} \mathbf{r}_{ij} \mathbf{F}_{ij} \right\rangle_{r<r_c} + \Delta p, \quad (5)$$

and the potential energy of liquid is obtained by

$$E_p = \left\langle \sum_{i=1}^N \sum_{j>i} \varphi_{ij} \right\rangle_{r<r_c} + \Delta E_p. \quad (6)$$

The values,  $\Delta p$  and  $\Delta E_p$  in Eq.(5) and (6), respectively, are correction terms which occur by cutting off the effect of the potential at  $r = r_c$ . Simulations are carried out from  $t = 0$  to  $t = 10$  with temperature control and from  $t = 10$  to  $t = 50$  without temperature control in order to create an equilibrium state at temperature  $T$ . The data are sampled from  $t = 50$  to  $t = 200$ .

In Kataoka's method, the excess Helmholtz free energy  $A^e$  (after subtracting the ideal gas term) is given as follows:

$$\frac{\beta A^e}{N} = \sum_{n=1}^5 \sum_{m=-1}^5 A_{mn} \left(\frac{\rho}{\rho_o}\right)^n \left(\frac{\beta}{\beta_o}\right)^m, \quad (7)$$

where  $\beta = 1/kT$ . The values  $\rho_o$  and  $\beta_o$  are used in order to nondimensionalize the coefficient  $A_{mn}$  in Eq. (7) and are given by  $\rho_o = 1/\sigma_m^3$  and  $\beta_o = 1/\varepsilon_m$ , respectively. The excess potential energy,  $E_p$ , and pressure,  $p$ , are obtained by

$$\frac{\beta E_p}{N} = \beta \left\{ \frac{\partial}{\partial \beta} \left( \frac{\beta A^e}{N} \right)_{\rho} \right\}, \quad (8)$$

$$\frac{\beta p}{\rho} - 1 = \rho \left\{ \frac{\partial}{\partial \rho} \left( \frac{\beta A^e}{N} \right)_{\beta} \right\}. \quad (9)$$

Using these equations, the coefficient,  $A_{mn}$ , is determined so that the pressure and potential energy obtained from Eqs. (7), (8) and (9) are consistent with the results of MD simulations. In this paper 284 state points of liquid oxygen are simulated at various temperatures and densities. In a previous paper, it was reported that the temperature and pressure of the system are greatly changed when the system changes in two phases (Kinjo and Matsumoto 1998). In the present paper, the MD results in which the difference between simulated and given temperature is larger than 5% of the given temperature are considered to be in two phases and are excluded from the data to calculate the coefficient,  $A_{mn}$ . The state points inside the spinodal line are also excluded because they are also considered to be in two phases. Moreover, the state becomes solid at lower temperature and higher density. In this paper, the mean square displacement of each system is calculated and the MD results in which its mean square displacement is less than  $5 \sigma_m$  are also excluded because they are considered to be solid. Figure 3 shows the simulated state points and obtained spinodal line of the monatomic liquid and the diatomic liquid. The spinodal line shows the TLM of the liquids. In this

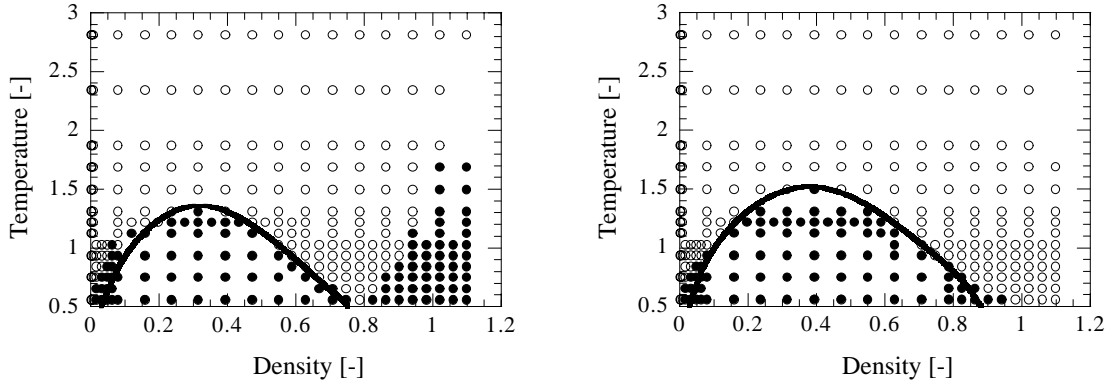


Figure 3: Simulation points and spinodal line: (Left) Monatomic liquid, (Right) Diatomic liquid.

figure, the density and temperature are reduced by  $m/\sigma_m^3 = 1.276 \times 10^3 \text{ kg/m}^3$  and  $\varepsilon_m/k = 1.063 \times 10^2 \text{ K}$ , respectively. The white circles show the MD results which are used to calculate the EOS and the black circles show those which are excluded. Figure 4 shows the spinodal line of the monatomic liquid and that of the diatomic liquid obtained by each EOS. As shown in this figure, the TLM of the diatomic liquid shifts to a higher density and a lower pressure than that of the monatomic liquid. This is caused by the fact that the diatomic liquid has a lower pressure than that of the monatomic liquid as the density increases. The virial term, the second term of Eq.(5), is expressed using the radial distribution function  $g(r)$  by

$$B = \frac{1}{3V} \left\langle \sum_{i=1}^N \sum_{j>i}^N r_{ij} \left( -\frac{d\psi_m(r_{ij})}{dr_{ij}} \right) \right\rangle_{r<r_c} = -\frac{1}{6} \rho^2 \int_0^{r_c} r \frac{d\psi}{dr}(r) \cdot g(r) 4\pi r^2 dr. \quad (10)$$

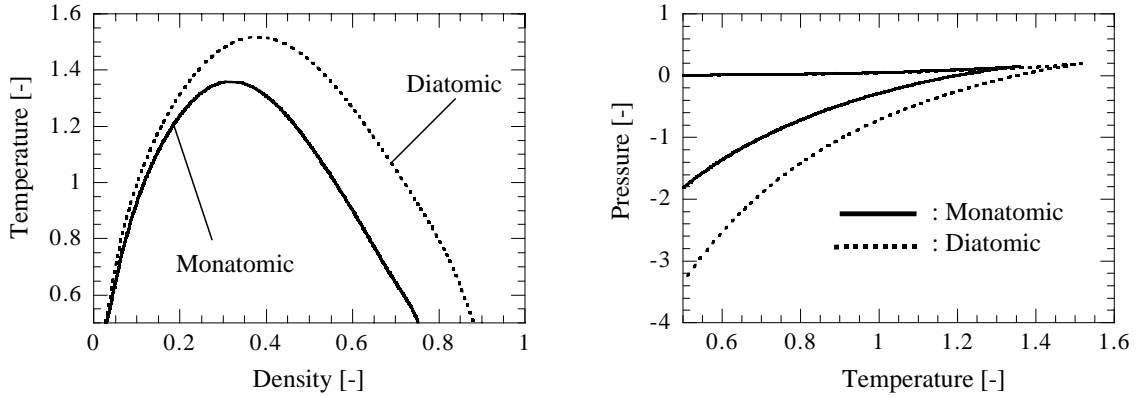


Figure 4: Spinodal line of monatomic and diatomic liquid: (Left) Density–temperature curve, (Right) Pressure – temperature curve.

The monatomic and the diatomic liquid are simulated at the state of  $T = 1.0$ ,  $\rho = 0.8$  in order to obtain the averaged virial or the radial distribution function in these liquids. The number of molecules is taken to be  $N = 6912$ . The averaged virials of monatomic and diatomic liquids are shown in Fig. 5 and their radial distribution functions are shown in Fig. 6. The averaged virials of monatomic and diatomic molecules with regard to the orientation obtained in the same manner as the potential mentioned in Sec. 2 are also shown in Fig. 5. As shown in Fig. 5 the averaged virial of diatomic molecules with regard to the orientation is

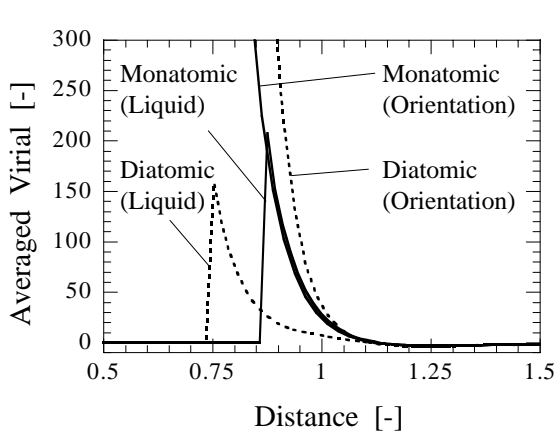


Figure 5: Averaged virial in each liquid

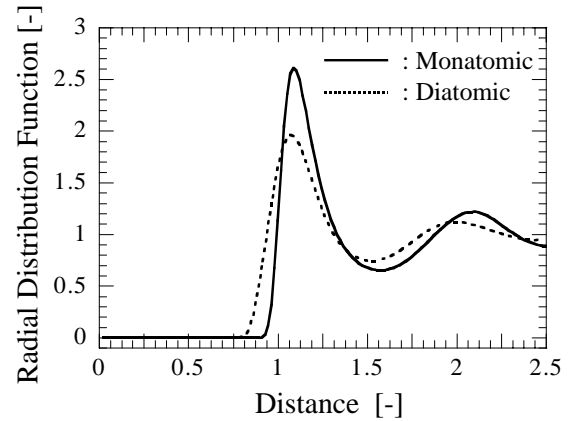


Figure 6: Radial distribution function in each liquid

larger than that of monatomic molecules. However, the averaged virial in the diatomic liquid is smaller than that in the monatomic liquid in spite of the fact that the distance between molecules in the diatomic liquid is less than that in the monatomic liquid. It is also shown in these figures that the virial of monatomic molecules is consistent with the averaged virial in the monatomic liquid because the virial of monatomic molecules is the function of only the distance of molecules. However, the averaged virial in the diatomic liquid is much different from the averaged virial of diatomic molecules with regard to the orientation and is much smaller than the averaged virial in the monatomic liquid at a distance of  $r < 1.1\sigma_m$ . This is because the orientation of diatomic molecules are not isotropic and diatomic molecules obtain stable orientations at which molecular potential force is lower at the distance of  $r < 1.1\sigma_m$ . The pressure of the diatomic liquid, therefore, becomes smaller than that of the monatomic liquid. Moreover, this effect is greater as the density of the liquid is higher. For this reason, the minimum pressure point, i.e., TLM, shifts to a higher density

and a lower pressure.

## 4 Kinetic Limit of Metastability

Bubbles are formed at a density higher than the TLM at a certain temperature owing to the density fluctuation when the density of the liquid becomes less than a certain value. The point is the kinetic limit of metastability (KLM) and in classical nucleation theory this point is predicted from the balance of forces acting on a bubble and the probability of the density fluctuation in liquid (Blander and Katz 1975). Moreover, it has been reported that pure liquids have an obvious KLM (Kinjo and Matsumoto 1998). In this paper, bubble nucleation in monatomic and diatomic liquids are simulated in order to investigate the effect of the internal degree of freedom on the KLM. Unlike the TLM, the KLM cannot be defined by the EOS. In this paper, microcanonical MD simulations are performed at a certain temperature by changing density, and the KLM at this temperature is defined as the minimum density at which bubbles are not generated. The number of simulated molecules is 10,976. A periodic boundary condition is imposed. The initial position and velocity of molecules are given as mentioned in Sec. 3. Simulations are carried out with the temperature being controlled from  $t = 0$  to  $t = 10$  and without control from  $t = 10$  to  $t = 50$  to obtain equilibrated configurations. These configurations are expanded uniformly and instantaneously from  $\rho_{ini}$  to  $\rho_{fin}$  with certain expansion ratios. During this process the system temperature decreases. Therefore, the simulations are carried out with the temperature being controlled from  $t = 50$  to  $t = 60$  to recover the temperature of the system and the simulations are continued to  $t = 200$  to observe the bubble nucleation. These simulations are carried out by increasing  $\rho_{fin}$  by 0.01 from the TLM at a certain temperature, and the minimum density at which bubbles are not generated is defined as the KLM at that temperature. Bubble nucleation in monatomic liquid and the time history of pressure are shown in Fig. 7, where  $T = 1.0$ ,  $\rho_{ini} = 0.80$  and

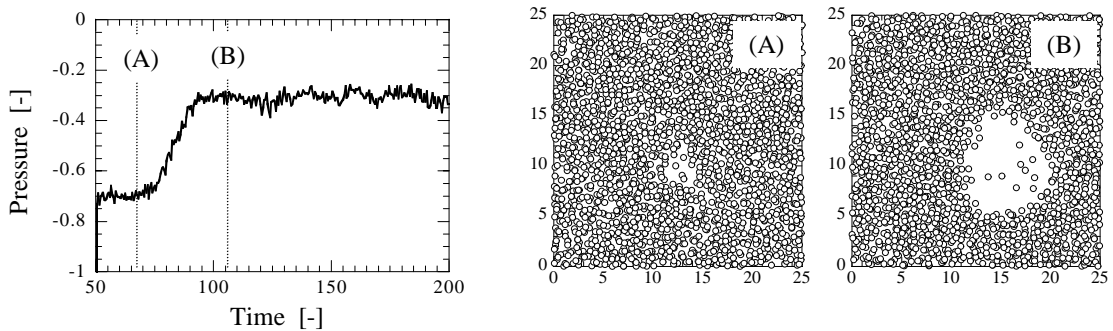


Figure 7: The change of pressure against time and snapshots of the bubble formation

$\rho_{fin} = 0.62$ . In this figure the simulation domain is divided into five sections and only the section in which the bubbles are clearly apparent is shown. As shown in this figure, bubbles are not generated as soon as the pressure decreases, and the density fluctuates till the point of (A). At this point, the local density becomes less than the critical value and bubbles are generated with a rapid pressure increase. In this paper, the degree of density fluctuation against the density of liquid is investigated. The probability of the number of neighboring molecules which exist in the distance of  $r_c$  from a certain molecule is defined as the characteristic of the density fluctuation. When the liquid is homogeneous, it has been reported that the probability is a normal distribution whose average is  $\langle n_o \rangle$ , the averaged number density of liquid (Hoheisel 1992). The deviation of the distribution corresponds to the density fluctuation in the liquid. The probability of the number of neighboring molecules by changing the density at a constant temperature  $T$  is shown in Fig. 8. The temperature of the system is  $T = 1.0$  and the densities are  $\rho = 0.65$ ,  $\rho = 0.75$  and  $\rho = 0.85$ . As shown in this figure, the deviation of the normal distribution becomes small as the density of the liquid increases.

Table 1 shows the TLM and KLM of monatomic liquid and diatomic liquid at  $T = 0.9$ ,  $T = 1.0$  and  $T = 1.1$ . As shown in this table, the difference between TLM and KLM of the diatomic liquid is larger than that of the monatomic liquid, and therefore it is considered that the density fluctuation in the diatomic liquid

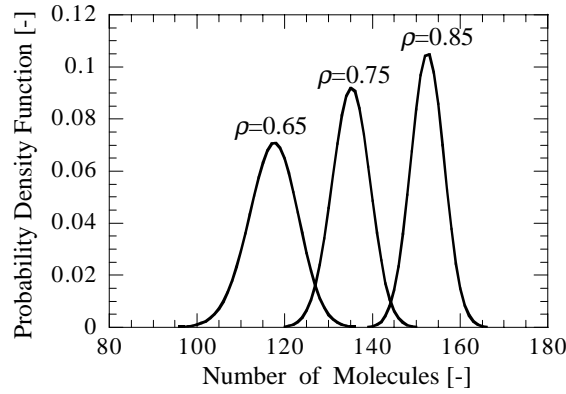


Figure 8: The dependence of liquid density on the fluctuation of number of molecules.

is larger than that in the monatomic liquid. However, the density at the TLM of the diatomic liquid is higher than that of the monatomic liquid, and this result does not seem to be consistent with the result that the density fluctuation decreases as the density of the liquid increases. From these results it is considered that the molecular structure has some effects on the density fluctuation in the diatomic liquid, and therefore the density fluctuation in the diatomic liquid is larger than that in the monatomic liquid although the density of the diatomic liquid is larger. For this reason the density fluctuation of the monatomic and that of the

Table 1: The TLM and the KLM of monatomic and diatomic liquid oxygen

$T$		Monatomic		Diatomic	
		TLM	KLM	TLM	KLM
0.9	$\rho$	0.62	0.67	0.78	0.86
	$P$	-0.609	-0.569	-1.24	-1.10
1.0	$\rho$	0.59	0.63	0.75	0.82
	$P$	-0.403	-0.368	-0.903	-0.814
1.1	$\rho$	0.55	0.58	0.71	0.77
	$P$	-0.232	-0.199	-0.632	-0.579

diatomic liquid are investigated. The probability of the number of neighboring molecules in the monatomic and diatomic liquids are shown in Fig. 9 and the radial distribution functions of each liquid are shown in Fig. 10. The simulation conditions are  $T = 1.0$  and  $\rho = 0.85$ . As shown in this figure, the deviation of the probability of the number of neighboring molecules in the diatomic liquid is larger than that in the monatomic liquid at the same temperature and density. This means that the density fluctuation in the diatomic liquid is larger than that in the monatomic liquid. The difference between the two liquids whose respective averaged potentials are consistent with each other is caused by the fact that diatomic molecules move in liquid more freely than monatomic molecules by changing their orientation. In other words, the diatomic molecules can change the intermolecular potential by changing their orientation as shown in Fig. 2, and they can, therefore, exist in the region in which monatomic molecules cannot exist due to the strong repulsive forces by changing their orientation to decrease the repulsive forces as shown in Fig. 10. For this reason the diatomic molecules move more freely in liquid and therefore the density fluctuation is greater.

## 5 Conclusions

In this paper the thermodynamic limit of metastability (TLM) of monatomic liquid and that of diatomic liquid were compared and the effect of the internal degree of freedom on the TLM was investigated. Liquid

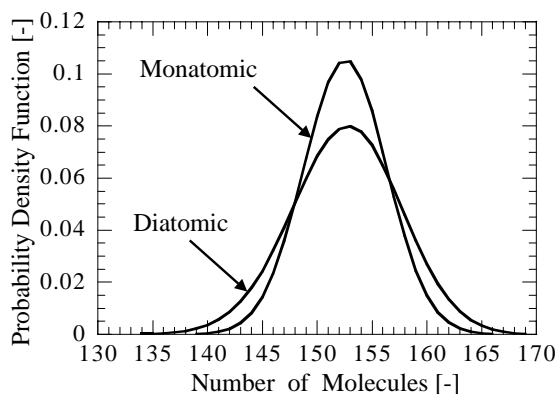


Figure 9: The probability density function of number of neighbor molecules around each molecule.

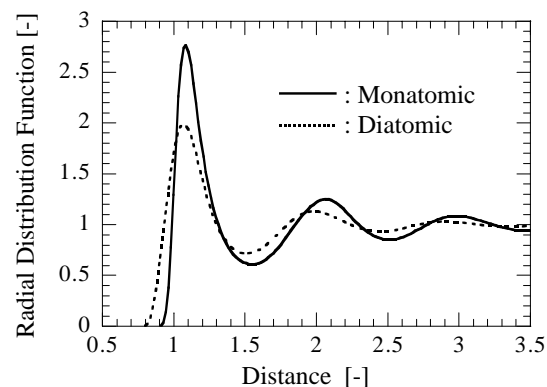


Figure 10: Radial distribution function of monatomic and diatomic liquid oxygen

oxygen was assumed as the simulated liquid. The Lennard–Jones (12–6) potential was used as the intermolecular potential for monatomic molecules and the 2 Center Lennard–Jones (2CLJ) potential was used for diatomic molecules. The potential parameters of the 2CLJ potential were set so that the averaged 2CLJ potential with regard to the orientation was consistent with that of the LJ potential. Using these potentials, the liquid at various temperatures and densities were simulated and from these data an Equation of State (EOS) for each liquid was obtained. From these EOSs the spinodal lines of each liquid were obtained and compared. It was found that the TLM of the diatomic liquid shifted to a higher density and a lower pressure compared with the monatomic liquid at the same temperature because the diatomic molecules had lower energy than monatomic molecules at  $r < 1.1\sigma_m$  due to a change in their orientation. Next, the kinetic limit of metastability (KLM) of each liquid was obtained from the various MD simulations and the effect of internal degree of freedom on the KLM was investigated. It was found that the difference between the TLM and KLM of the diatomic liquid was greater than that of the monatomic liquid. This was due to the fact that the diatomic molecules move more freely in the liquid by changing their orientation, and therefore the density fluctuation of diatomic liquid is larger.

## Acknowledgements

We would like to thank Associate Professor T. Ohara of the Inst. Fluid Science, Tohoku Univ. for helpful discussions and suggestions about this work.

## References

- Allen, M.P. and Tildesley, D.J., (1987). *Computer Simulation of Liquids*, Clarendon Press.
- Blander, M. and Katz, J.L., (1975). *AIChE J.*, **21**, 833–848.
- Hoheisel, C., (1992). *J. Chem. Phys.*, **97**, 2690–2693.
- Kataoka, Y., (1987). *J. Chem. Phys.*, **87**, 589–598.
- Kinjo, T. and Matsumoto, Y., (1998). *Fluid Phase Equilibria*, **144**, 343–350.
- Lin, L., (1998). *Microscale Thermophys. Eng.*, **2**, 71–85.
- Reid, R.C., Prausnitz, J.M. and Sherwood, T.K., (1977). *The Properties of Gases and Liquids, third edition*, McGraw–Hill.
- Singer, K., Taylor, A. and Singer, J.V.L., (1977). *Mol. Phys.*, **33**, 1757–1795.
- Tokumasu, T., Kamijo, K., Oike, M. and Matsumoto, Y., (2000) *Proc. ASME FED2000*, FEDSM2000-11019.
- Trevena, D.H., (1987). *Cavitation and Tension in Liquid*, Adam Hilger, Bristol and Philadelphia.